BRIDGING METHOXY GROUPS IN NaY, NaX AND NaLSX ZEOLITES

Vladimír BOSÁČEK[a,*], Stanislav VRATISLAV[b1] and Mája DLOUHÁ[b]

[a] *J. Heyrovský Institute of Physical Chemistry, Academy of Sciences of the Czech Republic, 182 23 Prague 8, Czech Republic; e-mail: vladimir.bosacek@jh-inst.cas.cz*

[b] *Faculty of Nuclear Sciences and Physical Engineering, Czech Technical University, 115 19 Prague 1, Czech Republic; e-mail: [1] vratisla@troja.fjfi.cvut.cz*

Received November 14, 2003
Accepted March 23, 2004

Distribution of chemisorbed methyl groups and sodium cations in the structure of NaY, NaX and NaLSX zeolites was estimated by neutron diffraction. Chemisorbed methyl groups were prepared in the structure by reaction of methyl iodide with reactive sodium cations available in SII and SIII positions of faujasites. Methyl cations CH_3^+, formed in the reaction, react immediately with the lattice oxygen forming surface bonded methyl groups in bridging configuration. ^{13}C NMR signals of chemisorbed surface species and their linear dependence on the intermediate electronegativity of the zeolite lie in the interval from 53 ppm for most basic CsLSX to 58 ppm TMS for stabilized and acid leached sample of H,NaY-St. Changes in the distribution of structural sodium cations in the lattice after chemisorption of methyl cations have been detected. C–O distances in surface methoxy groups in void cavities were longer than in ordinary crystalline organometallic compounds with bridging methoxy groups. The location of chemisorbed methyl groups at the O_1 lattice oxygen type was most probable for NaY. Nuclear densities of chemisorbed methyl groups were detected in NaX at O_1 and at O_4 lattice oxygens. The origin of the split signal at 58 ppm on NaX and NaLSX samples has been discussed.

Keywords: Zeolites; Cations in faujasites; Chemisorbed methylium cations; Neutron diffraction; ^{13}C MAS NMR spectroscopy.

The nature of acid or basic sites, their amount and distribution of their strength in the zeolitic lattice are widely discussed in the literature. IR and high resolution NMR (HR NMR) spectroscopy on solids contributed significantly to the analysis of absorption bands of the ν(O–H) vibration[1–5] and to the assignment of chemical shifts of ^1H signals[6–8], respectively. Experimental results[9–13] as well as theoretical investigations[1–5,14–18] demonstrated that chemical properties of hydrogens are controlled by actual basicity of the lattice oxygen atoms and by the nature of their bonds. For that reason, various types, above all terminal and bridging structural OH exhibiting different acidity, were found in solids. Consequently, it has been shown that dif-

ferences in hydrogen acidities are well understood in the frame of the concept that considers various oxygen basicities (nucleophilicities) depending on the geometry and bonding conditions of hydrogens[9,10,15–21]. Experimental support was obtained not only from the mentioned spectroscopic results, but also from diffraction methods, where in particular neutron diffraction provided direct evidence of the location of hydrogens in faujasites with various H^+/Na^+ ratio[9–12] or in other zeolites[22–24].

Studies of systems with participation of carbenium ions have recently revealed that organic cations like CH_3^+, $CH_3CH_2^+$ etc. are chemisorbed on the surface of aluminosilicates forming polarized, more or less covalently bonded, species which exhibit similar spectral properties to organic alkoxy compounds[25–27]. Chemisorbed methyl cations CH_3^+ (methylium) produced by heterolytic splitting of methyl iodide in the reaction with sodium (or other) cations or with acid hydrogens of various zeolites were described in[26,27]. The observed ^{13}C MAS NMR signals of methyl carbon correspond with the bridging form of chemisorbed methyl cations forming thus alkoxy-like species. This explanation is well in line with the confirmed existence of bridging methoxy groups in organometallic compounds[28–30] and also with the generally accepted concept of bridging structural OH groups in zeolites and other metallosilicates. The distribution of bridging methoxy groups is expected to be regular over the whole lattice in contrast to terminal methoxy groups located in the lattice defects and on the crystal external surface[31,32].

The aim of our study was to estimate the location of chemisorbed species in the lattice and to elucidate the role and participation of various lattice oxygen types in chemisorption of methyl cations. Because of the long lifetime of chemisorbed species at the lattice oxygen (of the order of milliseconds at room temperature), we have made an attempt to estimate regular distribution of cations and chemisorbed species over the lattice and to locate chemisorbed CH_3^+ ions at different oxygen atoms similarly to successful location of bridging protons in faujasites and other zeolites[9–13,22–24] by neutron diffraction with Rietweld refinement.

Well-developed crystals of NaY, NaX and NaLSX with high contents of sodium cations and with low contents of defects and decationization were used in this study. The reaction of methyl iodide with sodium cations was used for the preparation of anchored methyl groups in the structure of zeolites.

EXPERIMENTAL

The crystal structures of NaY and NaX zeolite with (and without) chemisorbed methyl cations (surface methyl groups) have been investigated by powder neutron diffraction and by high-resolution solid-state ^{13}C MAS NMR. Chemical composition of the unit cell of investigated dehydrated zeolites NaX and NaY was $Na_{80.0}Ca_{1.2}[(AlO_2)_{82.4}(SiO_2)_{109.6}]$ and $Na_{48.9}Ca_{1.6}[(AlO_2)_{52.1}(SiO_2)_{139.9}]$, respectively. NaLSX zeolite was the sodium form of a faujasite structure with the Si/Al ratio 1.

Samples for neutron diffraction and NMR experiments were prepared as follows: zeolite was dehydrated at 10^{-5} mbar in a glass vessel at 400 °C for 10 h. Powdered zeolite was then transferred under vacuum into a thin-glass cylindrical vessel (diameter 12 mm, height 35 mm), which was sealed off for the diffraction experiment. A portion of the same sample was sealed off under vacuum in another glass tube for MAS NMR measurement as described earlier[26]. Chemisorption of methyl iodide was carried out in a special all-glass device where the dehydrated and evacuated sample was exposed to a known amount of methyl iodide vapour. After adsorption, the sample was cooled with liquid nitrogen and the diffraction vessel was sealed off. The samples were heated before diffraction or NMR experiments at 160 °C for 2 h in order to accelerate the reaction of methyl iodide with sodium cations of zeolites. The diffraction vessel with powdered sample was then placed in a cryostat holder. The samples were loaded for diffraction experiments with CH_3I or with CD_3I (99% D, Aldrich). Methyl iodide was enriched before ^{13}C NMR measurement with a small amount of $^{13}CH_3I$ (99% ^{13}C, Aldrich) in order to increase the ^{13}C content in adsorbate and to facilitate the detection of chemisorbed species.

^{13}C MAS NMR spectra were measured on a Bruker DSX200 spectrometer equipped with a magic angle spinning probehead at 50.32 MHz. The standard pulse program for Hahn echo with proton decoupling and cross-polarization pulse program was used (for details see[26,31,33]). A rotor spinning frequency of 4.5–5 kHz was applied.

Neutron powder diffraction patterns were collected at 298 and 7 K on a KSN-2 diffractometer placed at the LVR-15 research reactor in Řež near Prague. This device was equipped with a close circuit liquid helium cryostat type CP-62-ST/5 (Cryophysics SA). When the 0.1362 nm wavelength was used, the resolution $\delta d/d = 0.00075$ was achieved (d is the interplanar spacing). Complete structural parameters were determined by Rietveld analysis of powder neutron diffraction data using the GSAS software package. Some experimental parameters of the neutron diffractometer KSN-2 and characteristic features of the refinement processing were published elsewhere[34].

RESULTS AND DISCUSSION

Adsorbed Species Detected by ^{13}C MAS NMR on NaY, NaX and NaLSX Zeolites

The preparation of chemisorbed methyl cations was successful with many cationic forms of zeolites by the reaction of methyl iodide with weakly bonded zeolitic cations (or acid hydrogens) according to Scheme 1.

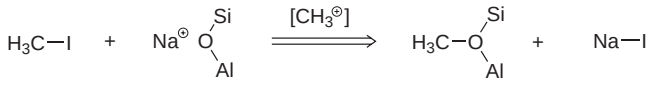

SCHEME 1

Heterolytic cleavage of methyl iodide produced CH_3^+ (methylium) and NaI species. The evolved methylium (an intermediate) reacts immediately with a nucleophilic lattice oxygen forming thus chemisorbed surface complex, which is similar to methoxy group in a bridging configuration. Let us stress that bridging surface methoxy compounds in zeolites exhibit ^{13}C MAS NMR spectra signals in the interval from 53 to 60 ppm TMS as published in[26,31–33]. This fact is documented for Y, X and LSX faujasites in Figs 1 and 2. ^{13}C MAS NMR spectra of chemisorbed CH_3^+ ions depicted in Fig. 1 for NaY exhibit a signal at 56 ppm (bridging methoxy group) and at –21 ppm (physically adsorbed unconverted methyl iodide). The corresponding spectra for NaX and NaLSX exhibit signals at 55 and 58 ppm and at 54 and 58 ppm, respectively. Both methoxy carbon signals are situated in the interval of bridging methoxy groups. The signal at 54 ppm corresponds with lattice oxygen of high basicity (nucleophilicity) and fits well the linear correlation dependence of chemical shift on the intermediate electronegativity S_{int} (Sanderson's definition) of various faujasite (shown in Fig. 2). These experiments clearly demonstrate the influence of the actual electronegativity of the lattice oxygen on the deshielding of the CH_3 carbon. The intrinsic basicity of the lattice oxygen decreases with increasing electronegativity and the deshielding of the methyl carbon increases. It follows from this experiment that the intrinsic basicity of the oxygen is dependent not only on the Si/Al ratio (S_{int} increases in the order: NaLSX < NaX < NaY, which modifies the oxygen basicity) but also on the nature of cations present in the lattice (see the orders of LSX, X and Y zeolites for Cs < Rb < K < Na < Li). The influence of the cation nature is involved in the intermediate electronegativities S_{int} of zeolites (via their atomic electronegativities) and, consequently, the intrinsic basicity of the lattice oxygen has been changed. Unfortunately, Sanderson's concept of intermediate electronegativity does not consider the influence of geometrical factors (differences in bond angles and lengths). This fact results in the hypothetical equal intrinsic basicity of all oxygen atoms in the lattice. This is, in fact, not true as follows from diffraction studies where different oxygen atoms (in faujasites of type O_1–O_4 in Fd3m) were estimated. Mortier et al.[17,18], in a theoretical attempt based on the advanced electronegativity equalization method (EEM), analyzed the intrinsic basicity of O_1, O_2, O_3 and O_4 using calculated charges and

Fukui functions at oxygen. Their conclusions are well in line with our observed trends in the chemical shift dependence on S_{int}. They also confirmed the possibility of differences in basicity of different types of lattice oxygen atoms. As the gradual decrease of oxygen basicity controls the increase in deshielding of the methyl carbon, we may expect an influence of oxygen basicity on the chemical shift of methyl carbon signal. As a rule, the ^{13}C

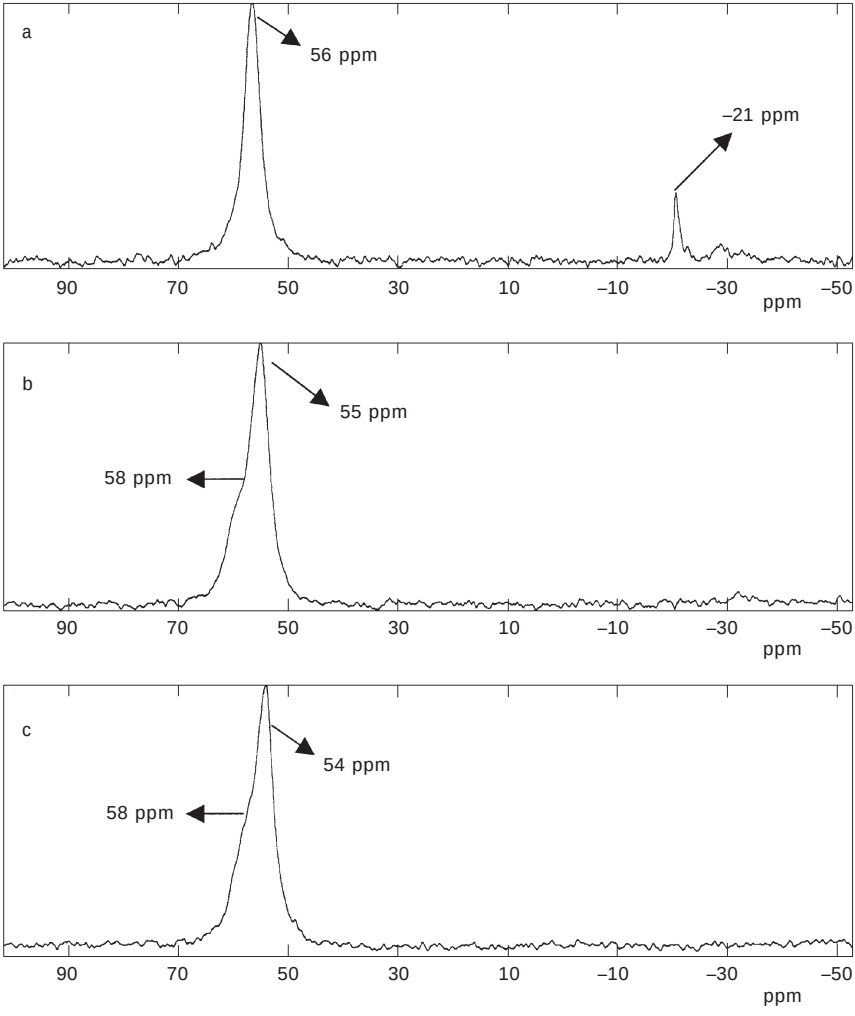

FIG. 1
^{13}C CP MAS NMR spectra of NaY (a), NaX (b) and NaLSX (c) with adsorbed methyl iodide after the treatment at 160 °C for 2 h

deshielding implies the increasing +δ charge at the methyl carbon[35]. A similar dependence of the ^{1}H MAS NMR chemical shift with electronegativity of oxygen is well known also for structure OH groups in zeolites[8,33,36].

The signal at 58 ppm (Fig. 1), the weaker shoulder, corresponds probably with more deshielded carbon of surface methoxy species. Unfortunately, this signal is situated above the regression straight line depicted in Fig. 2. Providing that the Sanderson electronegativity of all lattice oxygens is uniform, we should consider every deviation from the regression line as a deviation from our idealistic model. This has been suggested originally[26,33] to explain the 58 ppm signal with the bonds of CH_3^+ ions to a less basic lattice oxygen atom than in the case of the signal at 54 ppm. Such an explanation was in agreement with the fact that the 58 ppm signal would correspond (according to the linear dependence of the chemical shift on the intermediate electronegativity), with less basic lattice oxygen present e.g. in acid zeolites like ZSM-5 or ZSM-11. This explanation does not seem at first glance unrealistic, although the photoelectron spectroscopic studies[19] were not able to discover differences in oxygen 1s binding energies (ESCA) of different oxygen types in the same zeolite. However, in another study, Kaliaguine[20] observed, after deconvolution of the N(1s) peak of adsorbed pyridine or pyrrole, an indication of different basic sites. In order to exclude the effect of quadrupolar nuclei on the coupling with ^{13}C nuclei, a high magnetic field experiment was carried out. High magnetic field (11.7 T)

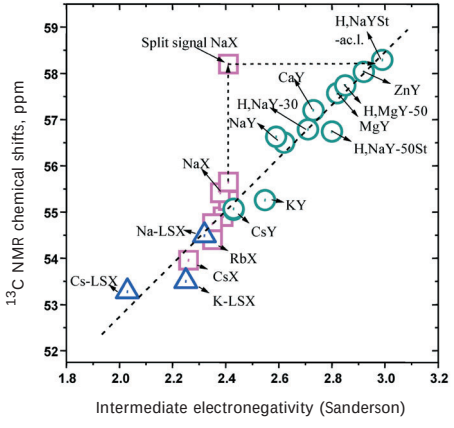

FIG. 2
The dependence of the ^{13}C NMR signal of bridging methoxy carbon on the intermediate electronegativity (Sanderson's definition)

(Fig. 3) improved the resolution of the split signal and, consequently, this experiment has shown that the signal at 58 ppm corresponds with Zeeman transition and not with electrostatic quadrupolar effects. Therefore, this signal was attributed to a special chemisorbed species in another bonding configuration characterized in ^{13}C NMR with different chemical shift. Nevertheless, as follows from the discussion in the following paragraphs, the situation is perhaps more complex because of the presence of other charged atoms in the vicinity. Let us note here that the all investigated samples of NaY (i.e. a faujasite without SIII cations in α-supercages), in contrast to NaX and NaLSX samples, exhibited in their ^{13}C MAS NMR spectra only one non-split bridging methoxy signal at 56 ppm together with a strong and narrow signal at –20.5 ppm of physically adsorbed unconverted methyl iodide (Fig. 1). It seems that the signal splitting effect may be associated with interaction of chemisorbed methyl groups with cations or with other charged species (e.g. iodine anion) inside the α-supercages.

Distribution of Cations in Dehydrated Zeolites and in Zeolites with Chemisorbed Species

Our structural parameters presented in Table I, part A for an initial dehydrated bare NaX sample are in agreement with the results refined in the Fd3 space group by Olson[37]. Parameters for characteristic chemisorbed sample are in the same Table I, part B. Parameters of the dehydrated NaY sample agree well with parameters refined in the space group Fd3m published

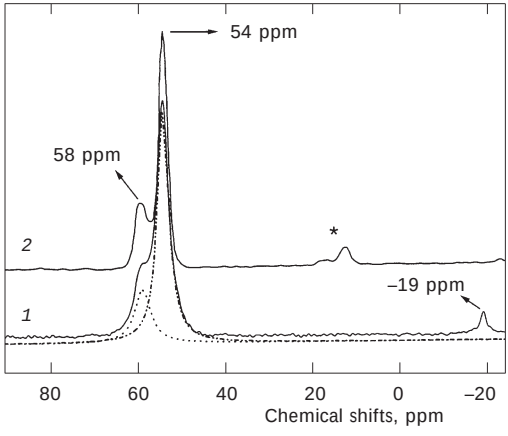

FIG. 3
^{13}C CP MAS NMR spectra of chemisorbed methyl iodide on NaX sample measured at magnetic field of 4.7 T (curve *1*) and 11.7 T (curve *2*)

TABLE I
Structural parameters for NaX samples. Final fractional coordinates[a] and standard deviations[b]

Atom	Site[c]	P^d	x	y	z	U_{iso}, Å^{2} [e]
A: NaX – dehydrated						
T1	96g	1.00	–0.05384(8)	0.12559(10)	0.03498(8)	0.011(5)
T2	96g	1.00	–0.05529(8)	0.03632(8)	0.12420(10)	0.012(6)
O1	96g	1.00	–0.1097(3)	0.0005(3)	0.1059(3)	0.022(5)
O2	96g	1.00	–0.0014(3)	–0.0021(3)	0.1418(3)	0.024(5)
O3	96g	1.00	–0.0366(3)	0.0729(3)	0.1796(3)	0.039(6)
O4	96g	1.00	–0.0691(3)	0.0729(3)	0.1796(3)	0.032(5)
Na1	16c	0.12(4)	0.0	0.0	0.0	–
Na2	32e	0.72(8)	0.0456(7)	0.0456(7)	0.0456(7)	0.058(9)
Na3	32e	0.19(8)	0.058(3)	0.058(3)	0.058(3)	0.061(9)
Na4	32e	0.98(3)	0.2294(2)	0.2294(2)	0.2294(2)	0.028(4)
Na5	96g	0.12(3)	0.421(3)	0.323(3)	0.160(3)	0.066(11)
Na6	96g	0.09(3)	0.435(3)	0.278(3)	0.167(3)	0.052(12)
Na6′	96g	0.10(3)	0.467(3)	0.314(3)	0.155(3)	0.057(11)
B: NaX with chemisorbed CH_3I						
T1	96g	1.00	–0.05420(8)	0.1261(10)	0.0351(8)	0.008(5)
T2	96g	1.00	–0.05589(8)	0.0362(8)	0.1242(10)	0.009(6)
O1	96g	1.00	–0.1103(3)	0.0006(3)	0.10620(3)	0.017(4)
O2	96g	1.00	–0.0012(3)	–0.0031(3)	0.1419(3)	0.015(5)
O3	96g	1.00	–0.03567(3)	0.0748(3)	0.0706(3)	0.018(6)
O4	96g	1.00	–0.0698(3)	0.0718(3)	0.1807(3)	0.019(5)
Na1	16c	–	0	0	0	–
Na2	32e	0.91(8)	0.0487(7)	0.0487(7)	0.0488(7)	0.035(7)
Na3	32e	–	0.0583	0.0583	0.0583	–
Na4	32e	1.01(3)	0.2306(2)	0.2306(2)	0.2306(2)	0.003(2)
Na5	96g	–	0.421	0.323	0.160	–
Na6	96g	–	0.435	0.278	0.167	–
Na6′	96g	–	0.467	0.314	0.155	–
Na7[f]	96g	0.28(3)	–0.209(3)	0.295(3)	0.088(3)	0.042(8)
M1[g]	96g	0.12(3)	–0.133(5)	0.193(5)	0.106(4)	0.067(9)
M2[g]	96g	0.12(3)	–0.133(5)	0.106(4)	0.193(4)	0.059(8)
I[h]	96g	0.26(3)	–0.217(5)	0.193(4)	0.193(4)	0.041(7)

[a] Origin at $\bar{3}$ of Fd3; A: a_o = 24.969(4) Å; B: a_o = 24.898(4) Å (reliability index R_{wp} = 6.21% and R_p = 4.97%). [b] Values in parentheses are the estimated standard deviations of the last digit. [c] Multiplicity and Wyckoff notation. [d] Occupation factor P. [e] Debye–Waller isotropic thermal factor U_{iso}. [f] Position not detected in the original evacuated NaX crystals. [g] M1 and M2 positions of the supposed chemisorbed methyl groups. [h] Position assigned to iodine in formed NaI clusters.

in[9,11,38] as discussed elsewhere[9,34]. Parameters of NaLSX (preliminary results presented in[39]) were refined in both recently discussed space groups[40–42] i.e. in the Fd3 space group and in the Fddd (orthorhombic) group but without any significant difference. Zeolite LSX (low silica X) has a Si/Al ratio of 1 and represents the highest number of charge-compensating cations of all faujasites. Cations are distributed over six possible sites as proposed by Olson[37] in the frame of the Fd3 space group. In recent publications[39,41,43–46], some results of which are collected in Table II, the distribution of Na or Li cation in faujasites was also tested by high resolution ^{23}Na (^{7}Li) MAS NMR. The NMR results altogether confirm the results from diffraction methods. It is clear that also our neutron diffraction results, presented in Table II, are well in line (considering various composition of materials and experimental deviations) with the observed cation distribution in all NaY, NaX and NaLSX samples published in literature.

Our experimental data allow to compare the changes in the occupation of positions of the lattice atoms in original evacuated NaX and in the same

TABLE II
Occupation of cationic sites per unit cell (p.u.c.) in dehydrated faujasites

Zeolite	Site	Type	Hunger[43,a]	Grey[44,a]	Olson[37,b]	Plevert[41,b]	Eulenberger[38,c]	Vratislav[d]
NaY	SI	16c	7	3			8	4
	SI′	32e	16	17			20	18
	SII	32e	30	30			30	32
NaX	SI	16c	4	2	3			3
	SI′	32e	16	28	29			29
	SII	32e	32	32	31			31
	SIII′(1,2)	96g	25	13	21			21
	SIII′(3)	96g	6	10	8			9
NaLSX	SI	16c	4			0[e]		0
	SI′	32e	18			32		25
	SII	32e	32			32		32
	SIII′(1,2)	96g	26			16		34
	SIII′(3)	96g	13			15		8

[a] NMR results. [b] X-ray diffraction. [c] Neutron diffraction. [d] Neutron diffraction, results of this study. [e] LiLSX diffraction data.

sample after chemisorption of methyl iodide. We observed serious changes in the distribution of the lattice elements after chemisorption of methylium ions. These changes were detected not only with occupation factors of cationic sites but sometimes also in coordinates of Na^+ cations. A typical example is depicted in Fig. 4a for NaX (without chemisorbed species) and Fig. 4b (with chemisorbed species), where a splitting (at 7 K) is demonstrated of the position SI' into two sites Na2 and Na3, which are separated at helium temperature but merged at room temperature (see also the section of faujasite depicted in Fig. 5). Similar effects, associated with migration of cations, were recently published by Grey et al. for strongly adsorbed fluorinated hydrocarbons[44] and calculated by Jaramilo et al.[47] On the other hand, cations in SII positions (e type in Wyckoff notation) are represented after chemisorption only with the fully occupied Na4 site (32 per unit cell), as follows from Table I, part B. Na4 (type e cations) as well as Na5, Na6 and Na7 (type g cations) take part in the reaction of CH_3I preferentially due to their easy accessibility in large α-supercages.

Structure and Location of Chemisorbed Methyl Cations CH_3^+ in Faujasites

The location of chemisorbed methylium ions was estimated from calculated Fourier maps of nuclear densities. In evaluation and analysis of data, some complications have arisen concerning the detection of a sufficient amount

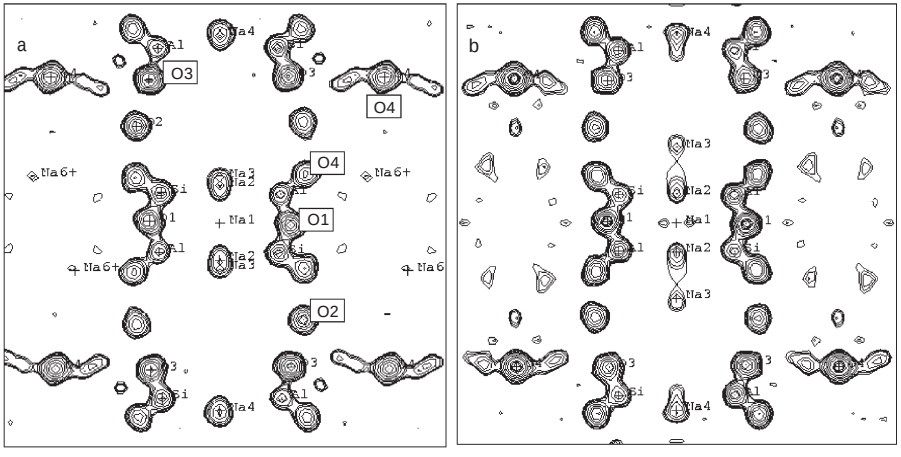

FIG. 4
Fourier maps of nuclear densities in the section plane along 3-fold axis (as depicted in Fig. 5) for dehydrated NaX (a) and NaX with chemisorbed methyl iodide (b) demonstrate the splitting of the Na2 and Na3 position after chemisorption

of chemisorbed methyl groups. This problem was pressing namely in Y zeolites where only SII cations (32 p.u.c.) are available for the reaction (Scheme 1) with adsorbed methyl iodide. It has been shown that after treatment at a higher temperature above 100 °C, the Na cations gain sufficient mobility and take part in the reaction with methyl iodide. From a differential Fourier map[34], as well as from the nuclear density map of perpendicular sections to the three-fold symmetry axis, it was concluded that chemisorbed species are probably located in large α-supercavity at the O_1 type of

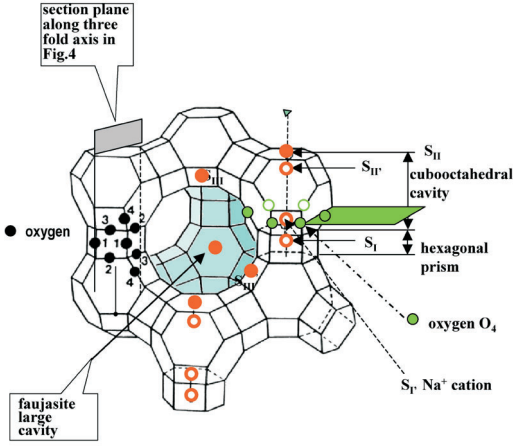

FIG. 5
Faujasite with section planes depicted in Fourier maps of nuclear densities (see Fig. 6)

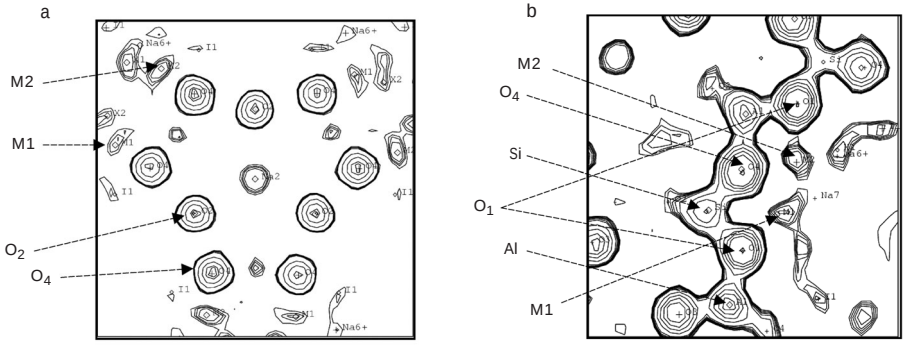

FIG. 6
Fouriere map of densities in a section plane perpendicular to [1,1,1] direction at the level of O_4 atoms after chemisorption of methyl iodide on NaX (a). A section plane with depicted Fourier nuclear density map of a chain of atoms O_4–Al–O_1–Si–O_4 etc. at the window of a supercavity (b)

lattice oxygen. While the low concentration of surface species made difficult their detection in Y structure, the situation in the case of NaX and NaLSX was better. Figure 5 demonstrates the situation in NaX zeolite where the plane of the section perpendicular to C_{3v} axis at the O_4 level is depicted (see density map a in Fig. 6). Such contours of nuclear densities were not detected in dehydrated NaX without chemisorbed substance[34] and we assign them to chemisorption complexes formed after the reaction (Scheme 1). This assignment was confirmed by parallel NMR analysis of the same sample where the formation of bridging methoxy species was proved. Another section (b) in Fig. 6 shows nuclear densities located at the chain of atoms forming the large window into an α-supercavity, such as O_4–O_1–O_4–O_1. In this section are visible also other nuclear densities of atoms situated near the section plane as Si, Al and also densities M1 and M2 assigned to chemisorbed methyl groups. Nuclear density contours at the O_4 oxygen denoted M1 and M2 are remarkable. Their estimated distances from the oxygen atoms are given in Table III.

Nuclear density maxima at O_1 and O_4 and densities assigned to Na7 and I (iodine anion) show that not only chemisorbed methyl but also the formed sodium iodide cluster as chemisorbed complexes may be depicted in Fourier maps. Although we should be cautious with the assignment and discussion of distances (due to low occupation factors) between oxygen and the observed maxima, let us try to turn attention to the observed fact that the M1–O_1 (or O_4) and M2–O_1 (or O_4) given in Table III are spread in the interval from 1.5 to 1.7 Å. It has been shown that in NaLSX the density M1 as well as M2 assigned to CH_3 exhibit a shorter distance to O_4 than to O_1, al-

TABLE III
Some important distances of chemisorbed methyl groups from lattice oxygen O_1 and O_4

Zeolite	Temperature K	Adsorbed CD_3I molecules p.u.c.[a]	M1–O_1 Å	M1–O_4 Å	M2–O_1 Å	M2–O_4 Å
NaLSX	298	24.8	1.627(6)	1.530(5)	1.656(6)	1.548(5)
	7	26.4	1.573(6)	1.535(5)	1.712(6)	1.572(5)
NaX	7	15.3	1.653(5)	1.764(4)	1.661(5)	1.789(4)
NaX(+Ar)	7	14.6	1.663(4)	1.670(4)	1.556(5)	1.572(5)
NaY	7	12.0	1.696(6)			

[a] Adsorbed molecules per unit cell of the crystal.

though in NaX structure the situation is inverse. It is assumed that this effect is associated with the amount of particles in supercages. Also an experiment with argon, which was subsequently adsorbed after preparation of surface methyl groups and which filled the supercages and restrict the movement of CH_3, has shown a weak decrease in M–O_i distances. Comparing this distance with the published C–O bond length for bridging methoxy group, e.g. in dimethylaluminium methoxide trimer (d = 1.436 Å)[29] or in trinuclear methoxy-bridged Ti–Mg complexes (d = 1.417 Å)[28] exhibited by compact nonporous crystals, it is clear that the distances observed by us in microporous crystals are longer than the C–O bond length estimated in nonporous crystals. To discuss this problem, it would be necessary to take into consideration at least two factors: (i) rotation and precession mobility of the C–O bond of anchored methyl group, and (ii) interactions of methyl hydrogens (or D atoms) with other species in their vicinity, e.g. with other lattice oxygen atoms. Fast reorientation at a higher temperature[41,42] may be the true reason for the unsuccessful determination of distinct positions of hydrogens (or D) in rotating methyl groups, which act in the *hkl* reflection plane as the mobile centre of gravity of CH_3 or CD_3 group. Although we have expected the immobilization of methyl groups at 7 K, we were unable to localize the positions of deuterium atoms as was performed in[48]. We assume that the detected nuclear density of protons (deuterons) exhibits higher uncertainty its position due to the disordered structure after relaxation. This results probably in uncertainty of density contour in space due to lower occupation of the site in contrast to normal lattice atoms. Nevertheless, the O–C distance lengthening may be also associated with the interaction of the considered chemisorbed CH_3 (or CD_3) group with other species. Under discussion are lattice oxygen atoms interacting via C–H←O< hydrogen bonding[48,49] (O< is skeletal oxygen) or interaction with other species like cations or iodide anions. It seems that in particular interaction in a cluster that consists of >O--[CH_3^+]--I^-Na^+ should be considered. Such a configuration may cause the lengthening of C–O bond due to competition of two bases (zeolitic oxygen and anion I^-). Let us only note that the calculated free surface methoxy groups in all quantum chemical approximations gave longer equilibrium C–O bond lengths 1.45–1.55 Å[39,45,46,50,51], than were the published experimental values, e.g.[28–30]. Further lengthening of the bonds may be possible only through strong intermolecular interactions[49,52–57] or under the influence of force field gradients in the zeolitic supercavities.

CONCLUSIONS

1. Chemisorbed methylium ions are located in the Y type faujasites structure at the lattice oxygen O_1 as bridging-type methoxy group characterized by a ^{13}C MAS NMR signal at 56 ppm.

2. Methylium ions are located in X faujasite at O_4 and O_1 lattice oxygen atoms only in α-supercavity. Although the location at two different sites corresponds well with two observed ^{13}C MAS NMR signals at 54 and 58 ppm of surface bridging methoxy groups, the existence of the signal at 58 ppm cannot be explained unequivocally. It may be considered as an effect of different oxygen basicities, or as a result of the interaction of methoxy group with other charged species in the supercavity.

3. Chemisorption of methylium ions at nucleophilic lattice oxygen sites has a remarkable effect on the distribution of cations in the lattice. This observed effect is in agreement with published similar effects of adsorbed polar molecules[44,47]. It demonstrates that long-range forces and variations of electrostatic field gradients significantly change the cations distribution.

Support of the Grant Agency of the Czech Republic (grant No. 202/2000/1427) as well as of the Czech Technical University, Prague (MSM 210000021) and the J. Heyrovský Institute of Physical Chemistry of the Academy of Sciences of the Czech Republic is acknowledged. Dr D. Kaucký is acknowledged for technical support and advice.

REFERENCES

1. van Santen R. A., Kramer G. J.: *Chem. Rev.* **1995**, *95*, 637.
2. Sauer J.: *Chem. Rev.* **1989**, *89*, 199.
3. Mortier W. J., Sauer J., Lercher J. A., Noller H.: *J. Phys. Chem.* **1984**, *88*, 905.
4. Senchenya I. N., Garrone E., Ugliengo P.: *J. Mol. Struct. (Theochem)* **1996**, *368*, 93.
5. Schroeder K. P., Sauer J., Leslie M., Catlow C. R. A., Thomas J. M.: *Chem. Phys. Lett.* **1992**, *188*, 320.
6. Pfeifer H.: *Colloids Surf.* **1989**, *36*, 169.
7. Brunner E.: *Microporous Mater.* **1993**, *1*, 431.
8. Hunger M.: *Catal. Rev.* **1997**, *39*, 345.
9. Jirák Z., Vratislav S., Bosáček V.: *J. Phys. Chem. Solids* **1980**, *41*, 1089.
10. Bosáček V., Beran S., Jirák Z.: *J. Phys. Chem.* **1981**, *85*, 3856.
11. Czjzek M., Jobic H., Fitch A. N., Vogt T.: *J. Phys. Chem.* **1992**, *96*, 1535.
12. Tao Sun, Seff K.: *J. Catal.* **1992**, *138*, 405.
13. Vitale G., Bull L. M., Powell B. M., Cheetham A. K.: *J. Chem. Soc., Chem. Commun.* **1995**, 2253.
14. Dubský J., Bosáček V., Beran S.: *J. Mol. Catal.* **1979**, *6*, 321.
15. O' Malley P. J., Dwyer J.: *J. Phys. Chem.* **1988**, *92*, 3005.
16. Kramer G. J., van Santen R. A.: *J. Am. Chem. Soc.* **1993**, *115*, 2887.

17. Uytterhoeven L., Dompas D., Mortier W. J.: *J. Chem. Soc., Faraday Trans.* **1992**, *88*, 2753.
18. Heidler R., Janssen G. O. A., Mortier W. J., Schoonheydt R. A.: *J. Phys. Chem.* **1996**, *100*, 19728.
19. Okamoto Y., Ogava M., Maezawa A., Imanaka T.: *J. Catal.* **1988**, *112*, 427.
20. Huang M., Adnot A., Kaliaguin S.: *J. Catal.* **1992**, *137*, 322.
21. Pingel U. T., Amoureux J. P., Anupold T., Bauer F., Ernst H., Fernandez C., Freude D., Samoson A.: *Chem. Phys. Lett.* **1998**, *294*, 345.
22. Fischer R. X., Baur W. H., Shannon R. D., Staley R. H., Abrams L., Vega A. J.: *Acta Crystallogr., Sect. B: Struct. Sci.* **1988**, *44*, 321.
23. Vitale G., Mellot C. F., Bull L. M., Cheetham A. K.: *J. Phys. Chem. B* **1997**, *101*, 4559.
24. Smith L. J., Davidson A., Cheetham A. K.: *Catal. Lett.* **1997**, *49*, 143.
25. Kazansky V. B.: *Acc. Chem. Res.* **1991**, *24*, 379.
26. Bosáček V.: *J. Phys. Chem.* **1993**, *97*, 10732.
27. Murray D. K., Chang J. W., Haw G. F.: *J. Am. Chem. Soc.* **1993**, *115*, 4732.
28. Chisholm M. H., Clark D. L., Hampden-Smith M. J., Hoffman D. H.: *Angew. Chem., Int. Ed. Engl.* **1989**, *28*, 432.
29. Gyepes R., Hiller J., Thewalt U., Polášek M., Šindelář P., Mach K.: *J. Organomet. Chem.* **1996**, *516*, 177.
30. Drew D. A., Haaland A., Weidlein J.: *Z. Anorg. Allgem. Chem.* **1973**, *398*, 241.
31. Bosáček V., Klik R., Genoni F., Spano G., Rivetti F., Figueras F.: *Magn. Reson. Chem.* **1999**, *37*(SI), S135.
32. Weitkamp J., Hunger M., Rymsa U.: *Micropor. Mesopor. Mater.* **2001**, *48*, 255.
33. Bosáček V.: *Z. Phys. Chem. (München)* **1995**, *189*, 241.
34. a) Vratislav S., Dlouhá M., Bosáček V.: *Physica B (Amsterdam)* **1998**, *241–243*, 400; b) Vratislav S., Dlouhá M., Bosáček V.: *Appl. Phys. A: Solids Surf.* **2002**, *74* (Suppl.), S1320.
35. Reed L. H., Allen L. C.: *J. Phys. Chem.* **1992**, *96*, 157.
36. Hunger M.: *Solid State Nucl. Magn. Reson.* **1996**, *6*, 1.
37. Olson D. H.: *Zeolites* **1995**, *15*, 439.
38. Eulenberg G. R., Shoemaker D. P., Keil J. G.: *J. Phys. Chem.* **1967**, *71*, 1812.
39. Vratislav S., Dlouhá M., Bosáček V.: *3rd European Conference on Neutron Scattering, Montpellier, France 2003*, Communication B54. *Physica B (Amsterdam)*, in press.
40. Porcher F., Souhassou M., Dusausoy Y., Lecomte C.: *Eur. J. Mineral.* **1999**, *11*, 333.
41. Plevert J., Di Renzo F., Fajula F., Chiary G.: *J. Phys. Chem. B* **1997**, *101*, 10340.
42. Feuerstein M., Lobo R. F.: *Chem. Mater.* **1998**, 2197.
43. Caldarelli S., Buchholz A., Hunger M.: *J. Am. Chem. Soc.* **2001**, *123*, 7118.
44. Grey C. P., Poshni F. I., Gualtieri A. F., Norby P., Hanson J. C., Corbin D. R.: *J. Am. Chem. Soc.* **1997**, *119*, 1981.
45. Oka H., Kasahara S., Okada T., Yoshida S., Harada A., Ohki H., Okuda T.: *Micropor. Mesopor. Mater.* **2002**, *51*, 1.
46. Feuerstein M., Engelhardt G., Mc Daniel P. L., MacDougall J. E., Gaffney T. R.: *Micropor. Mesopor. Mater.* **1998**, *26*, 27.
47. Jaramillo E., Auerbach S. M.: *J. Phys. Chem.* **1999**, *103*, 9589.
48. Carter V. J., Kujanpää J. P., Riddell F. G., Wright P. A., Turner J. F. C., Catlow C. R. A., Knight K. S.: *Chem. Phys. Lett.* **1999**, *313*, 505.
49. Chuvilkin N. D., Korsunov V. A., Kazansky V. B.: *Kinet. Katal.* **1986**, *27*, 1323.
50. Kitaigorodskii A. I.: *Molecular Crystals and Molecules*, Chap. 4. Academic Press, New York 1973.

51. Fyfe C. A.: *Solid State NMR for Chemists*, Chap. 8. University Press Guelph, Ontario 1984.
52. Shah R., Gale J. D., Payne M. C.: *J. Phys. Chem. B* **1997**, *101*, 4787.
53. Sinclair P. E., Catlow C. R. A.: *J. Chem. Soc., Faraday Trans.* **1997**, *93*, 333.
54. Corma A., Zicovich-Wilson C., Viruela P.: *J. Phys. Org. Chem.* **1994**, *7*, 364.
55. Blaszkowski S. R., van Santen R. A.: *J. Phys. Chem.* **1995**, *99*, 11728.
56. Aditya Bhan, Yogesh V. Joshi, Nicholas Delgass W., Thomson Kendall T.: *J. Phys. Chem. B* **2003**, *107*, 10476.
57. Stich I., Gale J. D., Terakura K., Payne M. C.: *J. Am. Chem. Soc.* **1999**, *121*, 3292.
58. Hriljac J. A., Eddy M. M., Cheetham A. K., Donohue J. A., Ray G. J.: *J. Solid State Chem.* **1993**, *106*, 66.
59. Mortier W. J., Van den Bossche E., Uytterhoeven J. B.: *Zeolites* **1984**, *4*, 41.